Case Studies in Thermal Engineering 6 (2015) 204–211

Contents lists available at ScienceDirect

Case Studies in Thermal Engineering

journal homepage: www.elsevier.com/locate/csite

Implementation variations of adiabatic steady PPDF flamelet model in turbulent H_2/air non-premixed combustion simulation

Qiong Li [a], Peiyu Zhang [b], Ying Feng [c], Peiyong Wang [c,*]

[a] College of Mechanical Engineering and Automation, Huaqiao University, Xiamen 361021, China
[b] School of Aerospace Engineering, Tsinghua University, Beijing 100084, China
[c] Department of Aerospace Engineering, Xiamen University, Xiamen 361005, China

ARTICLE INFO

Article history:
Received 24 August 2015
Received in revised form
21 September 2015
Accepted 7 October 2015
Available online 14 October 2015

Keywords:
PPDF flamelet model
Turbulent diffusion flames
Scalar dissipation rate
Lewis number effect
Opposed jet flame

ABSTRACT

Implementation of the adiabatic steady PPDF flamelet model involves a lot of variations including different scalar dissipation rate calculation methods and different mass diffusion models of the opposed jet flame. Four different look-up tables have been generated with the combinations of two different scalar dissipation rate calculation methods and two different mass diffusion models of the opposed jet flame. Simulation of a turbulent non-premixed H_2 jet flame is used to discriminate the accuracy of different implementation methods by comparison with experimental data. It is observed that the turbulent flamelets are very close to their equilibrium states and the simulation result is not sensitive to the choice of dissipation rate calculation method. However, the choice of mass diffusion model has significant influence on the simulation result and excluding the Lewis number effect should be enforced for the opposed jet flame simulation.

1. Introduction

The steady PPDF (Presumed Probability Density Function) flamelet model was invented by Peters [1] and it was based on the following assumptions: 1, the turbulent combustion is realized by numerous discrete steady laminar flamelets; 2, the flamelet thickness is less than the smallest length scale of turbulent flow field, i.e., the Kolmogorov length scale, so that the laminar flame structure could be preserved; 3, the turbulent eddy turn over time scale is much larger than the chemical reaction time scale so that the transient effect is negligible. This model has been implemented in major commercial CFD software such as Fluent, Star-CD, Star-CCM, and CFX; it has been used extensively in a lot of applications because it is fast with good convergence and reasonable accuracy.

In the adiabatic steady PPDF flamelet model, a turbulent flame is treated as an ensemble of discrete, adiabatic steady laminar flames, called flamelets. The individual flamelets are assumed to have the same structure as laminar flames in a simple configuration and are obtained mainly by simulation. The opposed jet flame [2] is commonly used to represent the laminar flame. The basic implementation method of the steady flamelet model is: (1) Calculate the turbulent flow field including the turbulent kinetic energy ke, its rate of dissipation ε, the average of mixture fraction $\bar{f}$ and its variance f''. The scalar dissipation rate at some location of the turbulent flow field is represented by $\overline{\chi_{st}} = C_\chi \varepsilon f''/ke$ where C_χ is a constant and is generally set to 2.0 [1]; (2) Construct an opposed jet flame with the scalar dissipation rate $\chi_{st} = \overline{\chi_{st}}$ and save the scalar

* Corresponding author.
E-mail address: peiyong.wang@xmu.edu.cn (P. Wang).

http://dx.doi.org/10.1016/j.csite.2015.10.001

result ψ_n of the opposed jet flame including temperature, species concentration, density, and other useful scalars as functions of mixture fraction $\psi_n(f)$. (3) The turbulence averaged scalars at this location of the turbulent flow field are calculated by statistically averaging of the opposed jet flame result $\overline{\psi_n} = \int \psi_n(f) P(f, \overline{f}, f'') df$ where $P(f, \overline{f}, f'')$ is the beta function shaped probability function [1]. In fact, the second step is often replaced by a table generation and looking up process: simulate a range of opposed jet flames with different scalar dissipation rates and construct a table $\overline{\psi_n}(\overline{f}, f'', \overline{\chi_{st}})$ in advance, and look up the table for the turbulence averaged scalars during the turbulent combustion simulation.

However, there are some variations in the model implementation which eventually influence the simulation accuracy of turbulent combustion, e.g. the choice of mass transport model of the opposed jet flame will influence flame temperature and flame structure of the opposed jet flame, the choice of scalar dissipation rate calculation method of the opposed jet flame will influence the match of the laminar opposed jet flame and the flamelet of turbulent combustion. Here, a non-premixed H_2 jet flame is simulated using the adiabatic steady PPDF flamelet model with the different implementation variations and the simulation results are compared with experimental data to identify the best implementation method.

2. Standard flame and CFD setup

The 100% H_2 fueled turbulent round jet flame is used here as the benchmark case. The detailed boundary condition and the experimental data including velocity profile, temperature profile, and species concentration profile are available online [3]. The fuel nozzle with inner diameter 3.75 mm injects pure H_2 at 296 m/s. Consequently, the nozzle Reynolds number is 10000. The velocity of co-flowing air is 1 m/s. The commercial software Star-CCM is used for the CFD simulation. The boundary condition has been set up according to the experimental boundary condition. The high Reynolds number K-Epsilon turbulence model is used for turbulence simulation. The transport properties are set to constant: dynamic viscosity 1.81E-5 PaS, thermal conductivity 0.0264 W/m/K, and species diffusivity 3.0E-5 m^2/s. The thermal radiation loss of H_2 flame is negligible and is ignored in the simulation, so the adiabatic steady PPDF flamelet model is appropriate.

Since the flame is axisymmetric, two-dimensional axisymmetric geometry is modeled. Fig. 1 shows the mesh and boundary setup. The axial domain covers 1450 mm and the radial domain covers 300 mm. The structured rectangular mesh contains 71820 cells (630 axial cell layers, 114 radial cell layers). The mesh size is not uniformly distributed and dense mesh is put in the region with strong gradients: 1 mm axial size is used for the 300 mm length next to the inlets, 2.5 mm axial size is used for the next 500 mm length, and 5 mm axial size is used for the rest 650 mm length. 0.625 mm radial size is used for the radius between 0 mm and 2.5 mm (fuel inlet+fuel pipe tip), 1.4844 mm radial size is used for the radius between 2.5 mm and 50 mm, 2.5 mm radial size is used for the radius between 50 mm and 150 mm, 3.947 mm radial size is used for the radius between 150 mm and 300 mm. The mesh independence has been tested by changing mesh density.

3. Opposed jet flame

Planar stretched laminar flames can be formed near the stagnation plane of two opposing jets. For a diffusion flame, the opposing jets supply fuel and oxidizer respectively. The flame structure is one dimensional and the scalars vary with the axial coordinate only. The PPDF flamelet model of turbulent combustion predicts finite rate chemistry effect by using the local stretch rate (or dissipation rate) to characterize local laminar flame structure (i.e., temperature, composition, density) and local extinction. The opposed jet flame is simulated with the OPPDIF package of Chemkin [4]. The real transport model includes the multi-component gas diffusion and the thermal diffusion of light species such as H_2 and H. The values of GRAD and CURV are set to 0.03, small enough to ensure that there are sufficient nodes and that the simulation result is independent of the number of nodes. Strict convergence criteria is also introduced to reduce computational truncation error. The fuel stream is pure H_2 and its temperature is 298 K, the oxidizer stream is air and its temperature is 298 K, the pressure is one atmosphere. The UCSD H_2 chemistry [5] is used here. The accuracy of this mechanism has been proved previously [6]. For a real H_2 laminar opposed jet flame, the preferential diffusion effect (H_2 mass diffusion is stronger than thermal diffusion), also called the Lewis number effect, exists and causes flame temperature higher than adiabatic equilibrium temperature (2389 K for stoichiometric H_2/air mixture) [2]. This phenomenon is true for individual flamelets inside turbulent

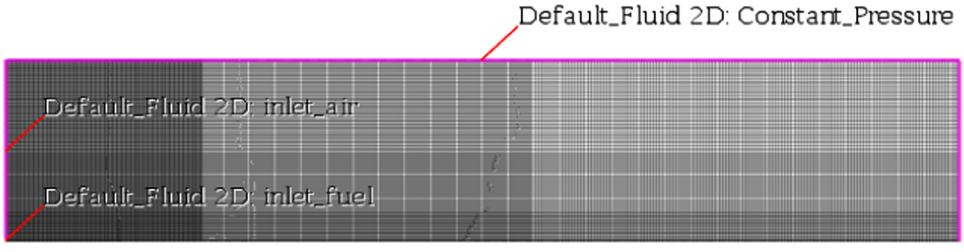

Fig. 1. Mesh and boundary setup for H_2 round jet flame simulation.

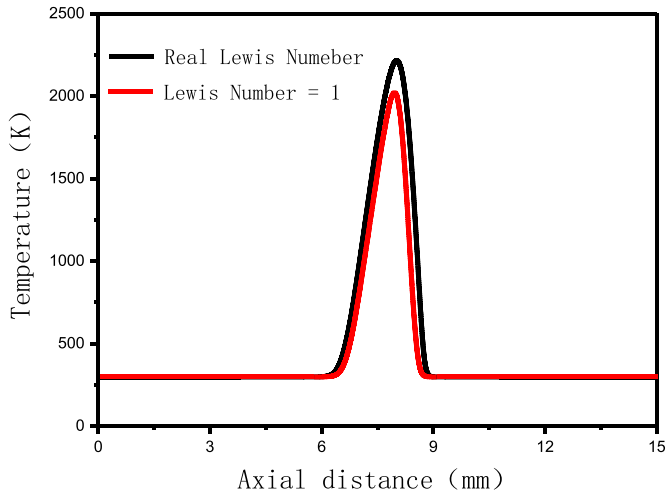

Fig. 2. Temperature profile comparison of the opposed jet flame with two different mass transport models.

combustion flow field, e.g., the measured instantaneous temperature in multiple points are higher than 2389 K; the measured highest instantaneous temperature is 2585 K in the turbulent H_2 jet flame [3], much higher than 2389 K. In the other hand, the steady PPDF flamelet model actually predicts the average temperature of an ensemble of flamelets, the average value might not show the preferential diffusion effect. Indeed, the measured peak average temperature of the round jet flame is 2173 K, much lower than 2389 K. So two mass transport model variations of the opposed jet flame simulation should be tested: 1, using the real multi-component mass diffusion model and considering the thermal diffusion of light species (The Lewis numbers of different species at different locations are different, it is marked as Real Lewis Number in Fig. 2); 2, setting the mass diffusivity of all species to local thermal diffusivity (The Lewis numbers of all species are 1 at all locations, it is marked as Lewis Number=1 in Fig. 2) and considering no thermal diffusion for any species. Fig. 2 shows the comparison of the simulated flame structure of the flame with stretch rate k=800 s^{-1} (The definition of stretch rate will be explained later) using the two different mass transport models. The flame with Lewis Number=1 is narrower meaning higher scalar dissipation rate and its flame temperature is lower because of no preferential diffusion effect.

4. Table generation

The stretch rate of the opposed jet flame is $k = 2/L[|V_O| + |V_F|\sqrt{\rho_F/\rho_O}]$; V_O and V_F are the velocity of the fuel stream and the oxidizer stream respectively, ρ_O and ρ_F are the density of the fuel stream and oxidizer stream respectively, and L is the distance between the nozzles. The opposed jet flame structure and temperature is independent on burner geometry and relies on stretch rate only. The steady PPDF flamelet table should include the flames with stretch rate from 0 s^{-1} to the extinction stretch rate. 42 opposed jet flames with the stretch rate k ranging from 4.44 s^{-1} to 18133 s^{-1} are calculated. The flame with stretch rate 18133 s^{-1} is an extinguished flame, the unstretched flame with k=0 s^{-1} could not be calculated with OPPDIF, it is calculated with the EQUIL package of CHEMKIN, the equilibrium state calculation code.

For each opposed jet flame, the sequential post processing steps are needed: mixture fraction calculation, scalar dissipation rate calculation, statistical average value calculation. The mixture fraction f is defined as the ratio of the mass from fuel stream to the total mass from both fuel stream and oxidizer stream. The mixture fraction is 1 at the fuel side and 0 at the oxidizer side, it varies continuously and monotonically across the opposed jet flame structure. The mixture fraction can be calculated with the species mass fraction: $f = (\alpha - a_O)/(\alpha_F - a_O)$; $\alpha = Y_{H2} - Y_{O2}/8$; the mixture fraction at the stoichiometric location where H_2 and O_2 are at stoichiometric condition and could be consumed completely ($\alpha = 0$) is $f_{st} = 0.0283$. With the definition of f, the original scalar variation (temperature, density, and species concentration) with the axial distance can be transformed to vary with the mixture fraction f, i.e., $\psi_n = \psi(f)$.

There are two ways to calculate the scalar dissipation rate at the stoichiometric location: 1, $\chi_{st} = 2D\,(\mathrm{d}f/\mathrm{d}z)^2_{st}$ where D is the mass diffusion coefficient and z is the axial coordinate of the opposed jet flame. There are multiple species at the stoichiometric location and their mass diffusion coefficients are different, it is hard to pick a mass diffusion coefficient, so the thermal diffusivity a is usually used to replace D, i.e., $\chi_{st} = 2\,a\,(\mathrm{d}f/\mathrm{d}z)^2_{st}$, the accurate thermal conductivity and specific heat calculation of the mixture is carried out with mixture averaging rules for mixture properties and temperature polynomial functions for thermal conductivity and specific heat of single species. 2, $\chi_{st} = k/\pi^* \exp(-2[\mathrm{erfc}(2f_{st})]^2)$ [1] (the original formula uses twice of the strain rate which is equivalent to stretch rate k). This formula is resulted from the analytical solution of the opposed jet flame with the assumption of a potential flow field with constant density and transport properties. The merit of this scalar dissipation rate calculation method is its simplicity, it does not require tedious calculation as in method 1; it has been adopted in FLUENT. In order to simplify the writing format of the two scalar dissipations rate

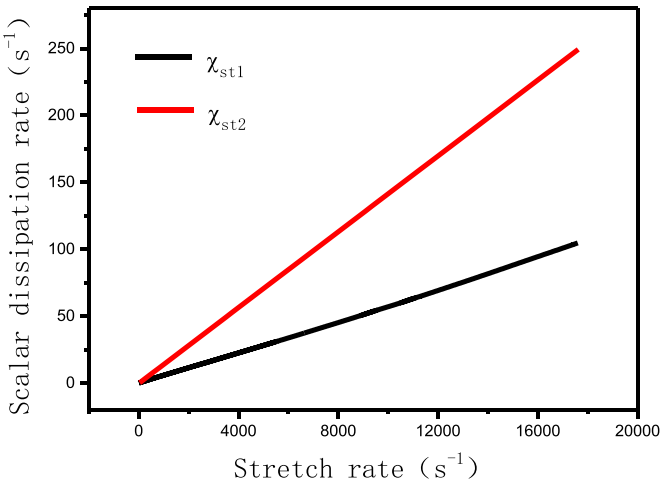

Fig. 3. Two types of scalar dissipation rate variation with stretch rate (multi-component mass diffusion model).

definitions, χ_{st1} and χ_{st2} are used to represent the first definition ($\chi_{st}=2\alpha\,(\mathrm{d}f/\mathrm{d}z)^2_{st}$) and the second one ($\chi_{st}=k/\pi^*\exp(-2[\mathrm{erfc}(2f_{st})]^2)$) in Fig. 3, respectively.

For each opposed jet flame (certain χ_{st}), 21 points are uniformly assigned for $f=0\sim f_{st}$ and $f=f_{st}\sim 1$ respectively, so total 41 points are distributed for $f=0\sim 1$. For each f value, its variation f'' could have any value between $0\sim f(1-f)$, this range is divided into 50 points. For each f and f'' combination, the corresponding scalars including temperature, species concentration, and density are calculated according the presumed beta probability density function. For $f''=0$, there is no need for the above statistical average calculation since there is no variation of mixture fraction and $\overline{\psi_n}=\psi_n(f)$ is used directly.

Putting all the data together following the organization rule of the Star-CCM software generates the look-up table: 43 flames with the scalar dissipation rate from 0 s^{-1} to the extinction value; for each flame, 41 points are used for $f=0\sim 1$; for each f, 50 points are used for $f''=0\sim f(1-f)$. Four tables are generated and used in the simulation separately to check the variation effect of the scalar dissipation rate definition and the Lewis number effect on the turbulent flame simulation: Table 1, multi-component mass diffusion model and thermal diffusion for light species, $\chi_{st}=2\,a\,(\mathrm{d}f/\mathrm{d}z)^2_{st}$; Table 2, Lewis number=1 for all species and no thermal diffusion for any species, $\chi_{st}=2\,a\,(\mathrm{d}f/\mathrm{d}z)^2_{st}$; Table 3, multi-component mass diffusion model and thermal diffusion for light species, $\chi_{st}=k/\pi^*\exp(-2[\mathrm{erfc}(2f_{st})]^2)$; Table 4, Lewis number=1 for all species and no thermal diffusion for any species, $\chi_{st}=k/\pi^*\exp(-2[\mathrm{erfc}(2f_{st})]^2)$.

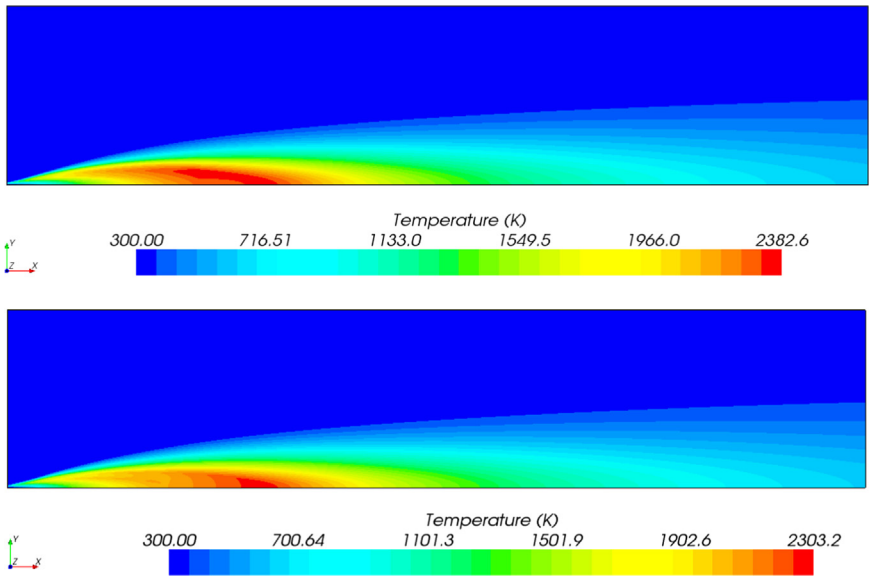

Fig. 4. Calculated temperature contour with Table 1 (up) and Table 2 (down).

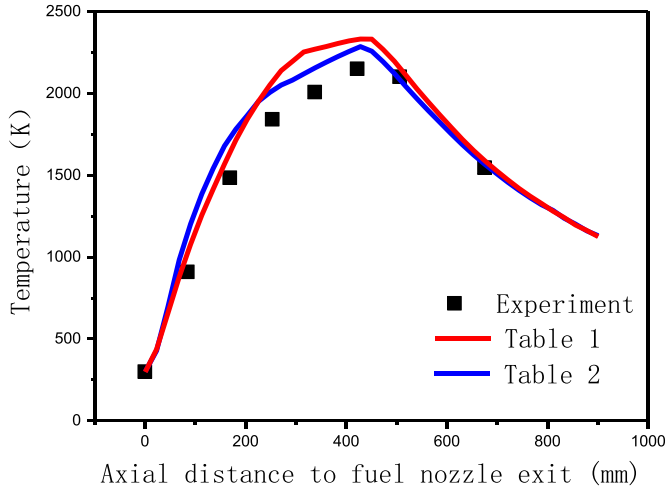

Fig. 5. Axial temperature profile comparison among experiment data and simulation data with Table 1 and Table 2.

5. Result and discussion

Fig. 4 shows that the simulations with Table 1 and Table 2 generate similar temperature contour and their main difference is the peak temperature, the peak temperature with Table 1 is 79.4 K higher than that with Table 2 since Table 1 is generated with the opposed jet flame considering the preferential diffusion effect (higher flame temperature). The predicted peak temperature of both cases are higher than the experimental data (2173 K). Fig. 5 and Fig. 6 show the axial temperature profile comparison and the radial temperature profile comparison at the axial location 337.5 mm above the fuel nozzle exit among the simulation results and the experimental data, respectively. It is clearly seen that the axial peak temperature with Table 2 (2286 K) is 135 K higher than the experimental data (2151 K) but it has better agreement with the experimental data than that with Table 1 (2332 K). The simulated radial temperature with Table 2 is also lower than that with Table 1 and it agrees better with the experimental data as shown in Fig. 6. This proves that the preferential diffusion effect should not be considered for the average temperature simulation. This is consistent with the measurement: the instantaneous temperature above the adiabatic equilibrium value is observed frequently, but the average temperature above the adiabatic equilibrium value is never found.

Since the preferential diffusion effect does not exist for average temperature, the simulation with Table 3 is not needed any more. The simulation result comparison with Table 2 and Table 4 are shown in Fig. 7 and Fig. 8. It is clearly seen that the choice of the scalar dissipation rate calculation method has negligible influence on the simulation result. Fig. 9 shows the predicted scalar dissipation rate contour. Most of the region has the scalar dissipation rate less than 0.04, a very small value. The opposed jet flame with the least nonzero scalar dissipation rate (0.047 s^{-1} and 0.065 s^{-1} according to the two different calculation methods) has the flame temperature 2340.2 K, very close to the equilibrium temperature 2389 K. In other words,

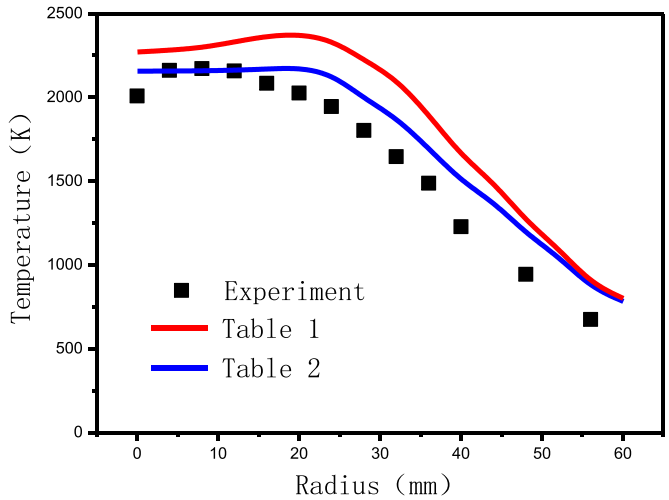

Fig. 6. Radial temperature profile comparison at the axial location 337.5 mm above fuel nozzle exit among experiment data and simulation data with Table 1 and Table 2.

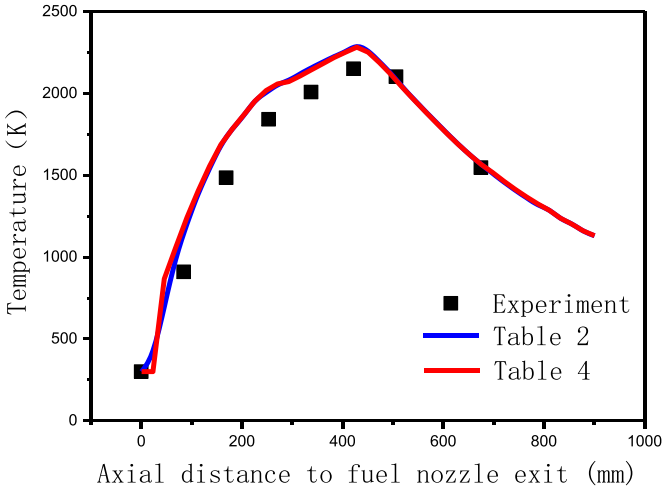

Fig. 7. Axial temperature profile comparison among experiment data and simulation data with Table 2 and Table 4.

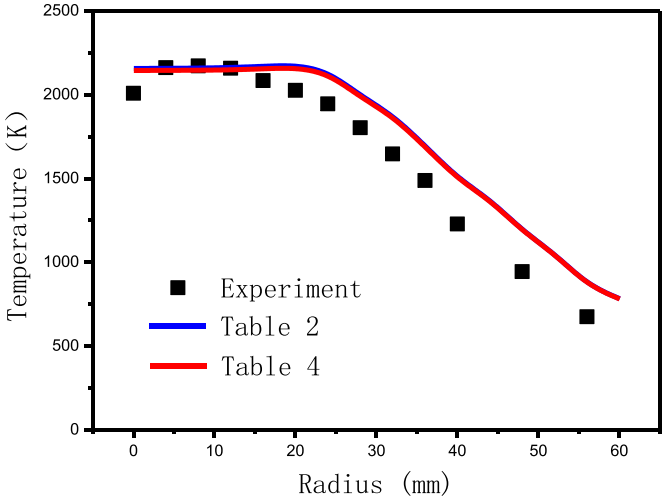

Fig. 8. Radial temperature profile comparison at the axial location 337.5 mm above fuel nozzle exit among experiment data and simulation data with Table 2 and Table 4.

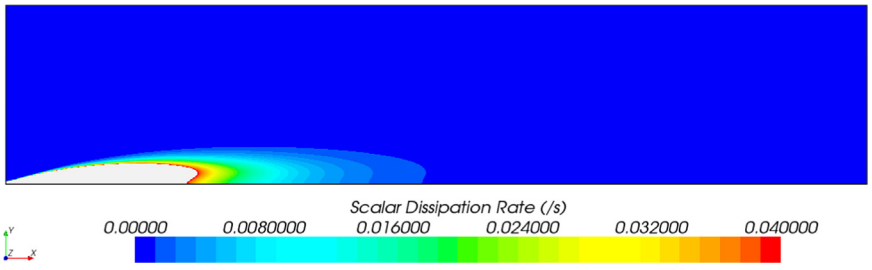

Fig. 9. Turbulent scalar dissipation rate contour.

the scalar dissipation rate in most of the flame region is almost 0 s^{-1}, the simulation gives very close result to that of the PPDF equilibrium model (similar temperature contour with the peak temperature 2303 K), so the PPDF flamelet model is not sensitive to the definition of the scalar dissipation rate for the tested case.

Although the adiabatic steady PPDF flamelet model predicts the flame temperature a little bit higher, it predicts the species concentration pretty well as shown in Fig. 10 and Fig. 11.

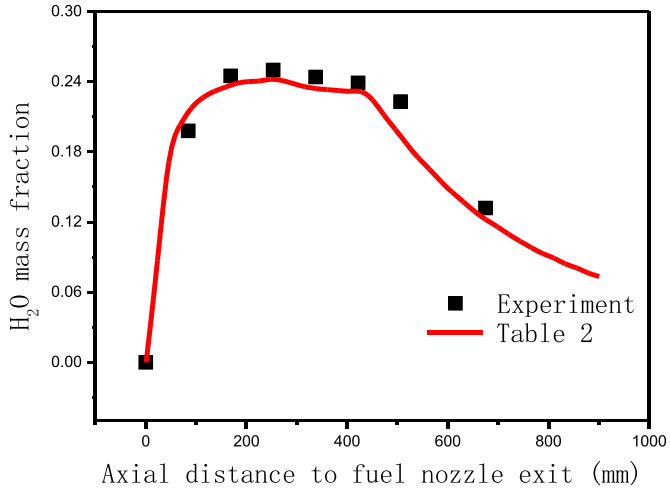

Fig. 10. Axial H_2O mass fraction profile comparison between experiment data and simulation data with Table 2.

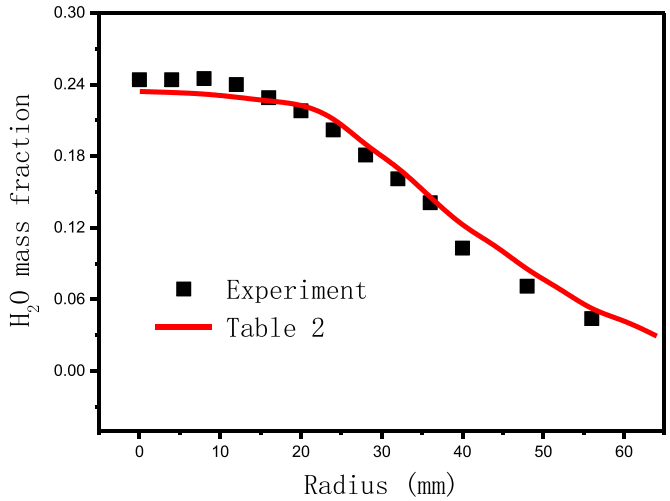

Fig. 11. Radial H_2O mass fraction profile comparison at the axial location 337.5 mm above fuel nozzle exit between experiment data and simulation data with Table 2.

6. Conclusions

The adiabatic steady PPDF flamelet model has been tested with the simulation of the turbulent H_2 round jet flame. Four PPDF flamelet tables with two variations of scalar dissipation rate calculation method and two variations of mass transport model of the opposed jet flame are generated. The following conclusions are obtained:

1. The Lewis number effect of the opposed jet flame should not be considered for the average temperature prediction of turbulent flames. Setting Lewis number = 1 for all species should be enforced in the simulation of the opposed jet flames.
2. The two types of scalar dissipation rate calculation methods do give out significantly different values, but the simulation result is not sensitive to the choice since the scalar dissipation rate is tiny in most of the flame region and the scalars are very close to the statistical average of their equilibrium state.
3. The adiabatic steady PPDF flamelet model over predicts the flame temperature for the tested case, but it predicts species concentration pretty well.

Acknowledgment

This work is sponsored by the National Natural Science Foundation of China Grant 51106131 and 51206057.

References

[1] Peters N. Turbulent combustion. Cambridge, UK: Cambridge University Press; 2000.
[2] R.W. Pitz, S. Hu, P. Wang, Tubular premixed and diffusion flames: effect of stretch and curvature, Progress in Energy and Combustion Science 42 (2014) 1–34.
[3] International Workshop on Measurement and Computation of Turbulent Nonpremixed Flames: ⟨www.sandia.gov/TNF/abstract.html⟩ (last accessed 18 Aug 2015).
[4] R.J. Kee, J.A. Miller, G. Evans, G. Dixon-Lewis, A computational model of the structure and extinction of strained, opposed flow, premixed methane-air flames, Proceedings of the Combustion Institute 22 (1988) 1479–1494.
[5] F.A. Williams, 2015. The San Diego Mechanism. Complete San Diego Mechanism: CK_2005-12-01, ⟨http://web.eng.ucsd.edu/mae/groups/combustion/mechanism.html⟩ (last accessed 18 Aug 2015).
[6] Q. Li, L. Fernandez, P. Zhang, P. Wang, Stretch and curvature effects on NO emission of H_2/air diffusion flames, Combustion Science and Technology 187 (2015) 1520–1541.